



Research Article

Behaviour of sintered fly ash aggregates and steel fibers on reinforced concrete slabs subjected to punching

Ranjith Babu B^{1*}, Thenmozhi R²

¹ Department of Civil Engineering, PSNA College of Engineering and Technology, Dindigul, Tamil Nadu (India), ranjithbabucivil@psnacet.edu.in

² Department of Civil Engineering, Government College of Technology, Coimbatore, Tamil Nadu (India), drthenmozhi@gct.ac.in

*Correspondence: ranjithbabucivil@psnacet.edu.in

Received: 21.03.2021; **Accepted:** 05.08.2022; **Published:** 30.08.2022

Citation: Ranjith Babu, B., and Thenmozhi, R. (2022). Behaviour of Sintered Fly Ash Aggregates and Steel Fibers on Reinforced Concrete Slabs Subjected to Punching. *Revista de la Construcción. Journal of Construction*, 21(2), 228-247. <https://doi.org/10.7764/RDLC.21.2.228>.

Abstract: In this study the optimum replacement percentage of sintered fly ash aggregates in M30 grade of concrete was identified based on 28 days cubical compressive strength value. The optimum replacement of Sintered Fly ash Aggregates (SFA) is 40 %. Before identifying the optimum replacement percentage, the SFAs were tested for suitability test such as crushing strength test, impact test and water absorption test. Further, the optimum 40 % SFAs in concrete is tested for punching shear on the Reinforced Concrete (RC) slabs for a dimension of 1000 mm x 1000 mm x 100 mm. In addition to know the effect of steel fibers in RC slabs subjected to punching. A hook ended steel fibers having an aspect ratio of 55, 80 and 100 is selected and varied by volume of concrete for the punching shear values on RC slabs. The RC slabs concrete contains aspect ratio of steel fibers 55 is varied for 0.25 %, 0.5 %, 0.75 % and 1 % for volume of concrete. In addition to that a constant volume of steel fiber 0.5 % is selected for the aspect ratios of 80 and 100 for the punching shear tests. The punching shear values for the RC slabs shows that partial replacement of SFAs and steel fibers in concrete enhances the punching shear strength. These experimental tested results are compared with finite element programming (ABAQUS) and international codes such as IS 456 and ACI 2011. The experimental punching shear results were higher when compared to international codes.

Keywords: Sintered fly ash aggregates, steel fibers, punching shear strength, ABAQUS, IS 456, ACI 2011.

1. Introduction

Managing industrial waste materials is one of the most important environmental issues. Concrete Technology can recommend some ways for reuse some industrial wastes such as fly ash (FA), silica fume (SF), and ground granulated blast furnace slag (GGBS). For the past two decades, usage of such minerals as a cement replacement material has been practiced by most of the invigilators. The concrete contains the aggregate made from municipal incinerated waste and Lytag (Commercial product name for sintered fly ash aggregate), shows that the Lytag aggregates proven that it is a better suitable for natural aggregates (Wainwright & Robery, 1997). The usage of sintered fly ash lightweight aggregates to produce concrete, needs to be more understanding on the properties of the aggregates and they also concluded that high volume of cementitious content leads to undesirable for the structural application. Addition of steel fiber reinforcement significantly increases the tensile

strength of lightweight aggregate concrete. The higher tensile strength together with low elastic modulus believed to be effective in reducing shrinkage cracking (Kayali, Haque & Zhu, 1999).

The pulverized fly ash as may be used up to 30% of cement replacement. However, utilization of industrial waste dust materials such as FA and GGBS in manufacturing of artificial aggregates attracted the invigilators and researchers as an alternative way to use in large (Kearsley, Wainwright & Amtsbuchler, 2005; Gesoğlu, Güneyisi, Mahmood, Öz & Mermerdaş, K, 2012; Cheeseman, Makinde, & Bethanis, 2005). The sintered fly ash aggregate concretes had higher compressive strength and modulus of elasticity than cold bonded aggregates (Kockal, & Ozturan, 2011). Concrete production using cold bonded and sintered fly ash aggregates, concluded the sintered fly ash aggregates had a better mechanical properties and higher durability factors (Güneyisi, E, Gesoğlu, M, Pürsünlü & Mermerdaş, 2013). The punching shear strength on reinforced concrete slabs using combined natural and clay aggregates, shows that the incorporation of rounded aggregates in concrete possess less punching angle compared to natural aggregate concrete and the study concluded that the round shape of aggregates provides higher restriction to punching (Youm, Kim, Moon, 2014 & Babu B, R, 2021).

The addition of pozzolanic materials like GGBS (Ground Granulated Blast Furnace Slag) increases the punching shear capacity of slabs by 21% in normal strength concrete (Nemani, Rao & Grandhe, 2016). The incorporation of lightweight aggregates in concrete produces reduction in self-weight of the structure and does not show reduction in aggregate interlock contribution in the punching zone (Caratelli, Imperatore, Meda & Rinaldi 2016). The partial replacement of natural coarse aggregates with recycled aggregates leads to reduction in stiffness, energy absorption and punching shear strength. The main reason for this was the replaced recycled aggregates were highly water absorption (Mahmoud, El tony, tony & Saeed, 2018). Mix design for production of concrete using sintered fly ash aggregates for the structural application based on tensile characteristics and also good in durability studies (Nadesan, & Dinakar, 2017).

The effect of sintered fly ash aggregates in concrete, they report that sintered fly ash aggregates improved the thickness and quality of ITZ (interfacial transition zone) with higher structural efficiency compared to normal concrete (Nadesan, & Dinakar, 2017). Research on punching shear strength of two-way reinforced concrete slabs is important to evaluate the safety in structural systems (Tuğrul Erdem, R, 2021). The flat slabs are supported directly on columns, without any intersection of beams between the columns. It generally transfers a significantly high concentrated load that acting on a relatively small area on the slab. Thus, the slab to column connection was a high concentration of shear stress. This localized stresses on the slab leads on punching risk. This phenomenon occurs suddenly (brittle fracture), which is why it has to be considered with careful design of slabs supported on columns only (e.g., in parking garages, office and residential buildings, bridges, etc.), but also in case of slabs lying below columns (e.g., foundation slabs or footings) (Bartolac, Damjanović & Duvnjak, 2015).

The volume of fibers (V_f) significantly affects the workability of the concrete mixtures. The most suitable value of V_f was in-between 0.5% to 2.5% by Volume of concrete (Shah, Daniel, Ahmad, Arockiasamy, Balaguru, Ball & Zollo, (1993). The increase in punching shear was due to the occurrence of steel fibers. It was primarily controlled by the volume fraction and aspect ratio of steel fibers (Harajli, Maalouf & Khatib, 1995). The addition of steel fibers in concrete is not only an effective way to improve its tensile stress, toughness and durability. The incorporation of steel fibers in slabs increases the ductility, load carrying capacity (Balendran, Zhou, Nadeem & Leung, 2002). The thickness design for the slab was based on post cracking behavior and concrete compressive strength (Kearsley, Elsabé & Elsaigh, 2003). The steel fiber was one of the most popular and widely used fibers in both research and practice (Mohammadi, Singh, & Kaushik, 2008). The steel fibers in concrete reduces the average crack width of the slab, increase initial stiffness and concrete ductility (Nguyen-Minh, Rovňák, Tran-Quoc & Nguyenkim, 2011).

The study of sintered fly ash aggregates in concrete is mostly in the forms of producing lightweight concrete and the failures in structural elements needs to be understood before using in to construction industry. Divyah N, Thenmozhi, R & Neelamegam M, 2020 studied the lightweight concrete made with sintered fly ash aggregate subjected to cyclic loading. Patra SN, Patra RK, Mukharjee BB, & Jena S, 2021 studied the partial replacement of sintered fly ash aggregate with natural aggregate with mineral admixture as metakaolin. This study shows that 30% sintered fly ash aggregate and 10-15% metakaolin

performs well and the structural evaluation of combined sintered fly ash aggregate and natural coarse aggregate studies are limited and this combination of aggregates are identified as a research gap.

In this present investigation the punching shear strength of the reinforced concrete slab is measured by identifying the optimum sintered fly ash aggregate in concrete and also by varying the volume of steel fibers in concrete with respect to the aspect ratio of steel fibers.

2. Materials and methods

The materials used in this work were Ordinary Portland Cement 53 (OPC 53), Chemical admixture (Conplast 430 sulpho-nated naphthalene), drinking water, natural sand, natural coarse aggregate and sintered fly ash aggregate (SFA) of 12.5 mm sieve passing, deformed high grade steel bars of 10 mm diameter with yield strength of 500 MPa and Hook ended steel fibers of aspect ratio 55, 80 and 100. Table 1 showed the properties of the steel fibers. Tests for the properties of the sintered fly ash aggregates were performed in compliance with Indian standard (IS 2386, 2002). The aggregates of Sintered fly ash were procured from GBC India private limited, Gujarat. The physical and mechanical properties of coarse aggregates used in this experimental system are shown in Table 2.

Table 1. Characteristics of hook ended steel fibers.

Aspect Ratio	Diameter (mm)	Length (mm)	Density (kg/m ³)	Tensile Strength (MPa)
55	0.55	30	7850	1450
80	0.75	60		
100	0.5	50		

Table 2. Physical and mechanical properties of natural and sintered fly ash aggregates.

Physical and mechanical properties	Natural aggregate	Sintered fly ash aggregate	Test methods
Specific gravity (Saturated surface dry)	2.65	1.4	IS :2386 (Part-3)
Water absorption for 24 h (%)	0.9	16.8	IS :2386 (Part-3)
Loose Bulk density (kg/m ³)	1490	830	IS :2386 (Part-3)
Rodded Bulk density (kg/m ³)	1626	895	IS :2386 (Part-3)
Fineness modulus	2.02	1.91	IS :2386 (Part-1)
Aggregate impact value (%)	19.42	27.78	IS :2386 (Part-4)
Aggregate crushing strength (%)	12.77	15.63	IS :2386 (Part-4)

2.1. Suitability level of sintered fly ash aggregates (SFAs) in concrete

To identify the better replacement level of SFAs in concrete. The SFAs were replaced (by weight) 20%, 40% and 60% in natural coarse aggregates. The mechanical properties of these mixes were designed for a grade of M30 (IS10262, 2009) and their properties were shown in Table 3. Based on the higher compressive strength of the concrete mixtures. The 40 % replacement of SFA was further investigated for punching shear strength on reinforced concrete slabs on the basis of steel fibers by varying volume and aspect ratio of steel fibers.

Table 3. Mechanical properties of SFAC mixtures.

MIX ID	Compressive strength ^a (MPa)	Split Tensile strength ^a (MPa)	Slump Value (mm)
M30	32.1	2.69	100
SFA20	34.40	2.80	140
SFA40	40.93	3.92	175
SFA60	35.73	3.09	205

^aTested values are average of 3 specimens; SFA, 20, 40 & 60 indicates the percentage replacement of sintered fly ash aggregates in concrete mixtures

2.2. Mix proportions of sintered fly ash aggregate concrete (SFAC)

Sintered Fly Ash Aggregates (SFAs) must be wetted in concrete before its application. If the SFAs is not moist, water from the paste will be absorbed, thereby losing its workability in fresh state and the effective water / cement ratio in the paste (Gomathi & Sivakumar, 2015) SFAs were held in water for 24hrs in this study and spread for four hours on a plastic sheet in free air before being used as Saturated Surface dry conditions (SSD). The concrete mixes were constructed in this test program according to Indian standard (IS10262, 2009). Seven concrete mixtures were developed for a 75-100 mm slump. Both blends employed the same volume of water and cement. The water-cement ratio was 0.35. Hook finished 25 percent volume steel fibers, 50 percent, 75 percent, and 100 percent with an aspect ratio of 55 in the concrete mixes. Likewise, for an aspect ratio of 80 and 100, 50 percent volume of hook-ended steel fibers were used. The mix ids and its average concrete mechanical properties are shown in Table 4.

Table 4. Fresh and hardened properties of SFAC mixtures.

MIX ID	Compressive strength ^a (f_{ck})	Split tensile strength ^a (f'_t)	Slump value (mm)
SFA40	40.93	3.92	175
SF4025	36.1	3.82	87
SFA4050	39.6	4.21	83
SFA4075	37.3	3.76	81
SFA40100	35.6	3.42	76
SFA405080	38.1	3.62	87
SFA4050100	36.2	3.53	96

^aTested values are average of 3 specimens; SFA4050 Indicates 40 % of sintered fly ash aggregate and 50 indicates the percentage of fibers.

2.3. Preparation of RC slab specimens

The slabs, supports, and loading system dimensions were the same in all of the test. The square plan dimensions of all the slabs were 1000 mm x 1000 mm and 100 mm thick. The slabs were casted by making a wooden ply wood as a formwork material. The slabs were provided with steel reinforcement at bottom, 10 bars of 10 mm diameter in both the spanning directions, with an effective concrete cover of 20 mm as shown in Figure 1. The steel bars were 900 mm long placed at 100 mm centre – centre distance. The slab specimens were cured with water after casting for 28 days. The slab specimens were coated with white paint, in order to ensure good identification of cracks during and after processing.

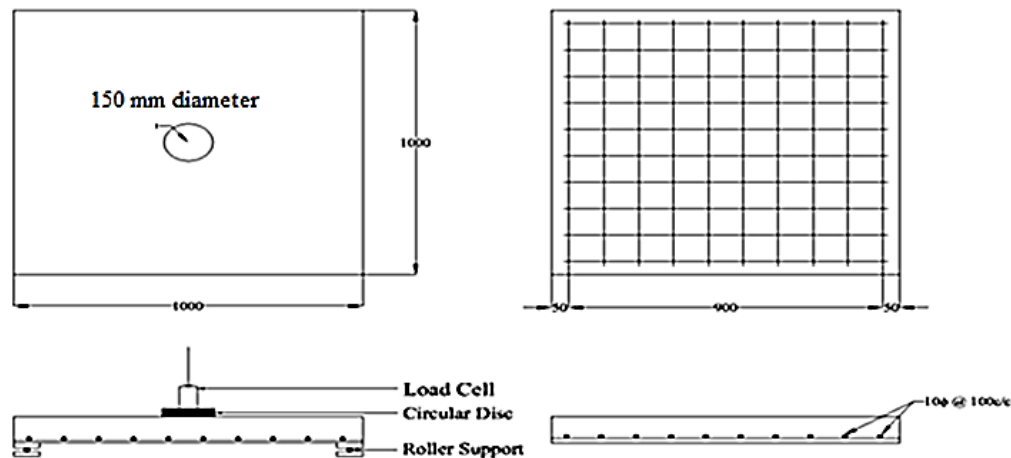


Figure 1. Experimental test setup and reinforcement detailing.

2.3.1. Loading arrangements, measurements and testing procedure

Figure 2 shows the selected restrained form. Researchers (Sermet & Ozdemir 2016, Reis, Brito, correa & Aruda 2015) have commonly used this form of restrained, and it reflects the general flat slab actions. The load cell recording the load and a plate of 150 mm diameter and 20 mm thickness were located from top to bottom of the hydraulic jack, respectively. Loading is carried out through the steel plate in the center of the slab. The Linear Variable Displacement Transducer (LVDT) was used for calculating slab deflection at mid-span. Measuring network of data loggers used to calculate loads and deflections. The load was applied up to 5 kN in increment. Deflections were reported via read out system during the study. The initiation and propagation of cracks were controlled at load intervals by visual inspection.



Figure 2. Loading arrangements for punching on a RC slab.

3. Experimental results and discussions

The load – deflection relationships for the tested slab specimens concrete having 40% of sintered fly ash aggregates and aspect ratio of steel fibers 55 were shown in Figure 3. From the load -deflection chart the ultimate load was nothing but punching shear strength of the slabs. The addition of steel fibers in concrete contains 40 % of sintered fly ash aggregates increases the punching shear values as 11.02 %, 10.23 %, 15.74 % and 28.34 %. As the fiber dosages increases the punching

shear strength increases linearly. In addition to that the presence of 40 % sintered fly ash aggregates made a better interlocking with the steel fibers and 60 % of natural aggregates.

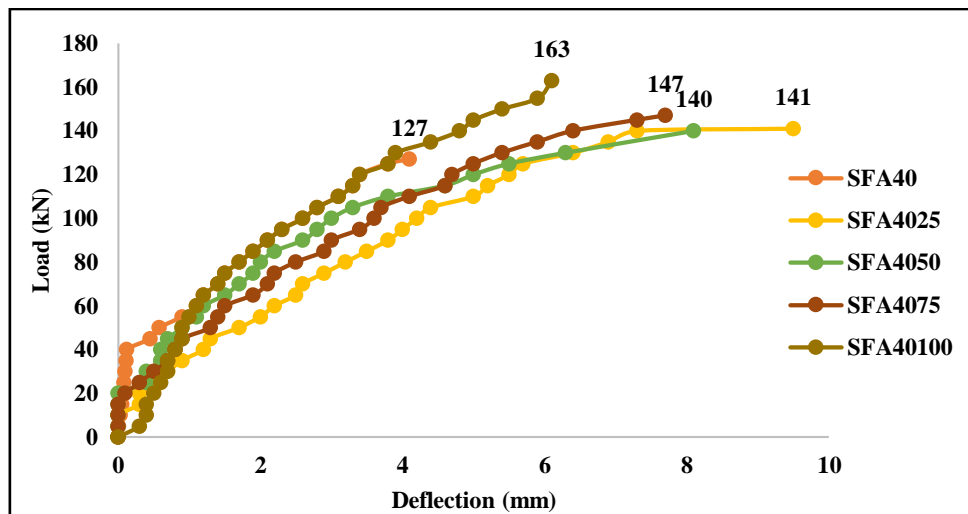


Figure 3. Load – deflection values for concrete contains steel fibers of aspect ratio 55.

The minimum volume of steel fibers added in concrete to increase the punching shear strength was 0.5 % in volume of concrete. To study this phenomenon with respect to aspect ratio of steel fibers. The 0.5 % volume of fibers were varied in steel fibers aspect ratio by 55, 80 and 100. The varied concrete slab specimens load – deflection values were shown in Figure 4. Compared to concrete slabs without fibers the aspect ratio 80 and 100 increases the punching shear strength by 51.18 % and 10.23 %. The concrete slab specimens carrying steel fibers of aspect ratio 55 and 100 got the same increased punching shear strength. This was due to larger length of the steel fibers for an aspect ratio of 100.

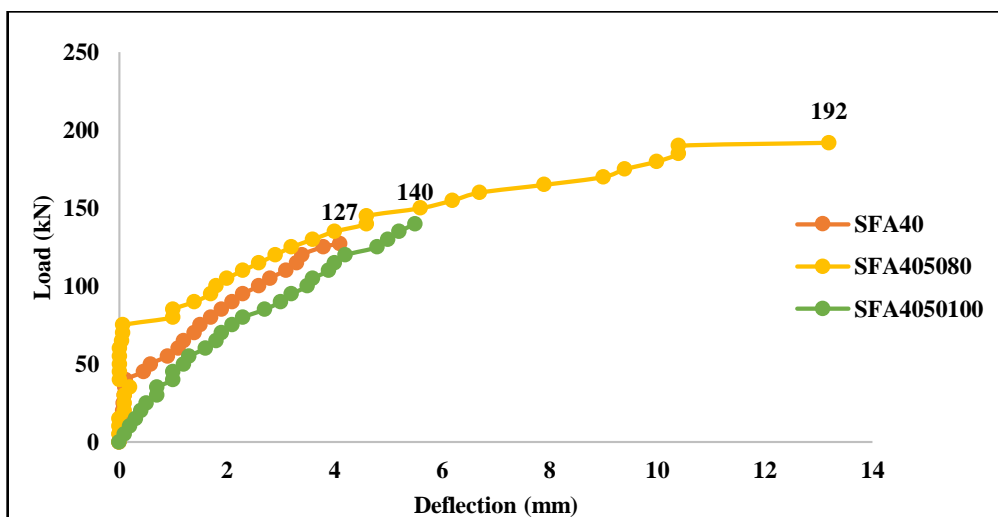


Figure 4. Load – deflection values for concrete contains steel fibers of aspect ratio 80 and 100.

3.1. Energy absorption capacity

Energy absorption is known as one of the toughness parameter measurements. In the case of concrete structures, the area under load-deflection curve for the slab specimens can be defined. Figure 5 displayed the measured energy-absorption values for each concrete mix.

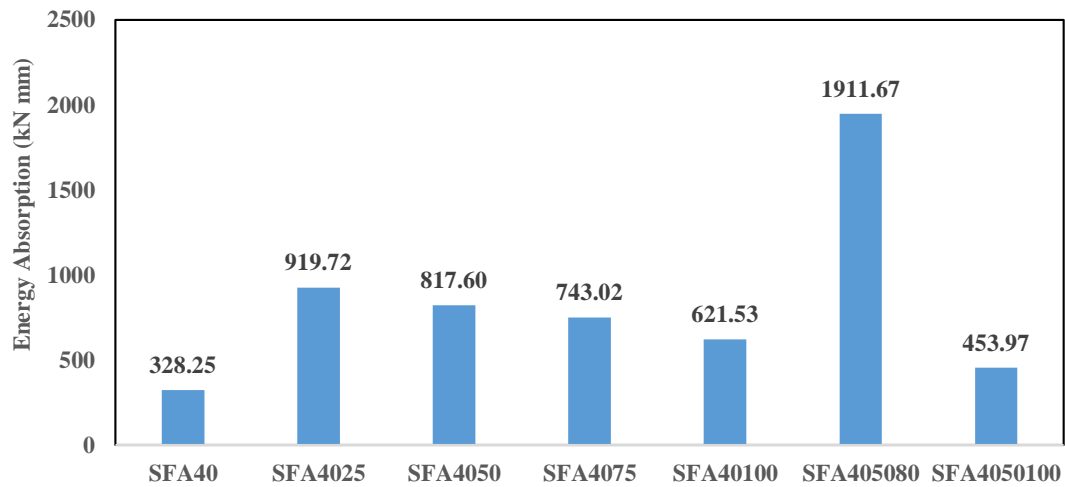
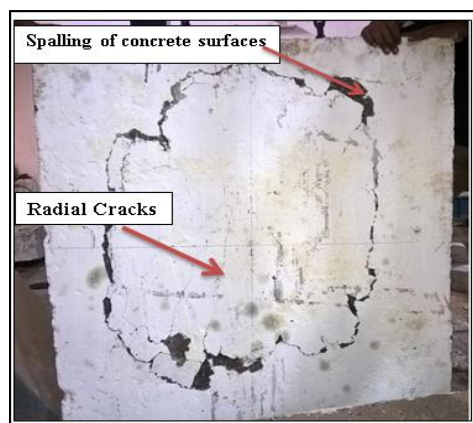


Figure 5. Energy absorption capacity of concrete mixtures.

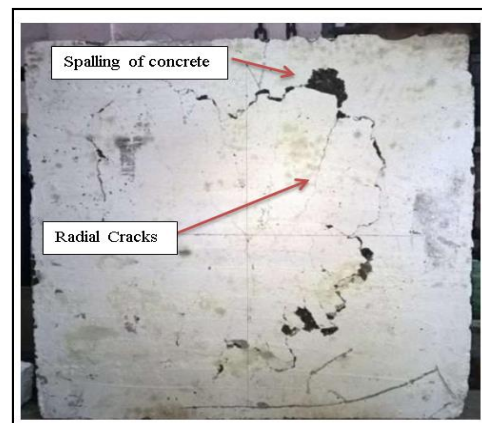
For each concrete mixture, the energy absorption potential has been increased as the amount of steel fibers only increases to 0.5 per cent. This amount of 0.5 per cent steel fibers was further varied with aspect ratio like 80 and 100. The normal concrete contains 40 percent of sintered fly ash aggregates from these energy absorption values and 0.5 percent of steel fibers having an aspect ratio of 80 were more resistant to punching shear force. The aspect ratio 100 provided less energy absorption compared with an aspect ratio of 55 and 80. It was concluded that 40 per cent of sintered fly ash aggregates need proper selection on the volume of steel fibers and the aspect ratio of steel fibers to increase the punching shear strength of concrete.

3.2. Cracking and failure pattern

Figure 6 displays the final crack patterns on all tested specimens. The cracks on the bottom sides are found to have been radial, mainly running between the loading point and the corners. A circular punching crack covering the load of patches occurred on the top surfaces and this was repeated with an expanded region on the bottom, clearly identifying the truncated cone. Similar pattern was reported by (Kuang & Morley, 1993) on the lightweight aggregate concrete having hook ended steel fibers. The failure modes of the slab were in the form of flexural failure when the concrete mixtures contain steel fibers. The addition of fibers can be taken as one such the way to improve the RC slabs against punching shear failure. This similar type of punching shear failure was attained where slab contains lightweight fiber reinforced concrete with ashes from municipal solid wastes (Caratelli, Imperatore, Meda & Rinaldi, 2016).



SFA40



SFA4025

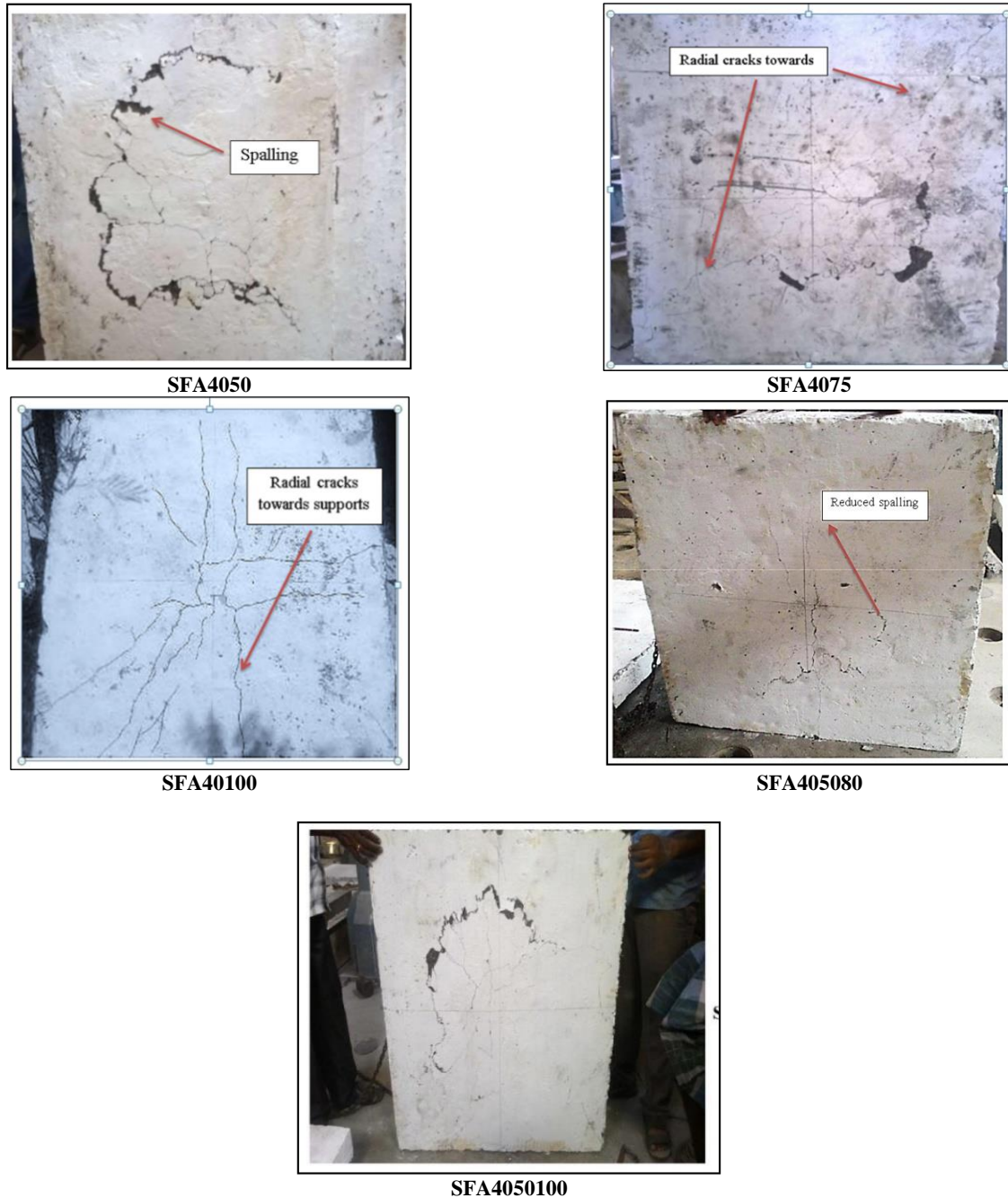


Figure 6. Failure patterns of slabs for different mixtures.

3.3. ABAQUS modeling and results

The Finite element analysis (ABAQUS) can be used as an assessment tool and it can provide insights into punching shear failure and crack formation. The slab model has been developed in the finite element-based software ABAQUS. This programme is capable of simulating a non-linearity material like concrete and steel material and it has been widely used for reinforced concrete structure's subjected to repeated loads and static loading. In order to simulate the tested slab, a full-scale

model was modelled using the ABAQUS Manual (2014). The loading disc was applied by a downward displacement experienced from experimental value, to simulate the real experimental behaviour. The modelled Reinforced concrete slab & loading disc were shown in Figure 7.

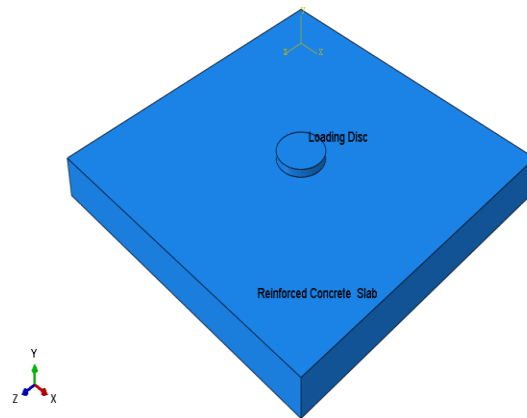
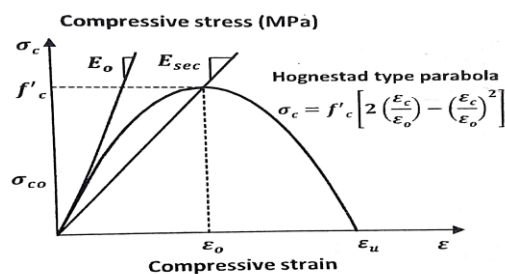


Figure 7. Geometry of the RC slab.

The concrete material properties used in the present analyses are: The initial tangent modulus, secant modulus, Poisson's ratio, compressive strength and split tensile strength for the selected concrete mixtures. The Poisson's ratio has to be taken as a constant value such as '0.2' for the cracked concrete. The dilation angle (ψ) 50, the shape factor (K_c) 0.667, the stress ratio (f_{b0}/f_{c0}) 1.16, Viscosity parameter (μ) 0.01 and the eccentricity (ϵ) 0.1. The f'_c was calculated based on compressive strength of the cubes as taken as $f'_c = 0.8$ times f_{ck} . The concrete compressive behaviour was derived with the help of Hognestad type parabola. The typical Hognestad type parabolic curve is shown in the Figure 8. This parabolic curve was based on initial modulus of elasticity (E_o) = $5500\sqrt{f'_c}$ and the Secant Elastic modulus (E_{sec}) = $5000\sqrt{f'_c}$. The linear branch ends at the 0.4 times the maximum stress value. The peak load corresponding strain $\epsilon_o = \frac{2f'_c}{E_{sec}}$.

Figure 8. Uniaxial compression stress – strain relationship for concrete. (Genikomsou & Polak, 2015)

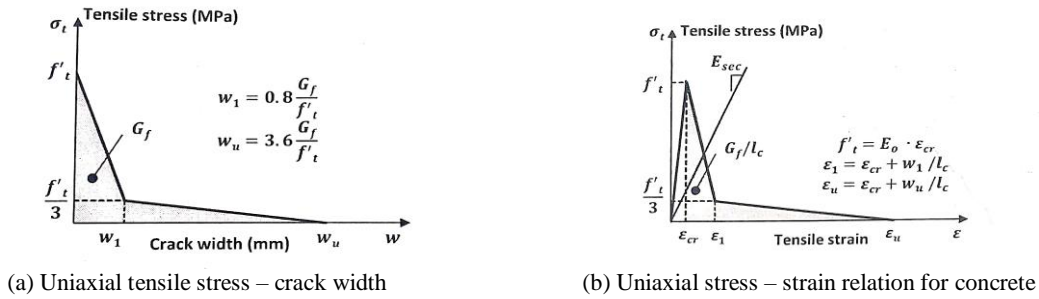


The tension stiffening curve was derived by making a tension stiffening curve with the help of fracture energy (G_f) values based on cylindrical strength of the concrete mixtures (f'_c) as shown in Equation 1. This equation was based on the CEB-FIB model code of version 2010. Where, characteristic length (l_c) was adopted as 20 mm. and f'_t was split tensile strength of the concrete mixtures.

$$G_f = 73(f'_c)^{0.18} \quad (1)$$

The tension stiffening curve was based on the bilinear stiffening response. The bilinear response of concrete and development of the curve model was shown Figure 9.

Figure 9. Development of tensile stress – strain model for concrete. (Genikomsou & Polak, 2015).



The uniaxial stress - strain relationship for steel reinforcement and steel disc was modelled with an elastic property of young’s modulus and Poisson’s ratio as 20000 MPa and 0.3 respectively. The plastic properties used for reinforced bar was shown in Table 5. The plastic properties were based on the tested results with a bilinear strain hardening yield stress – Plastic strain curve. An average mesh size of 20 mm was used to obtain the load – deflection curve. C3D8R has been used for concrete mesh, C3D8R has been used for steel bar mesh and C3D8R has been used for steel loading disc mesh.

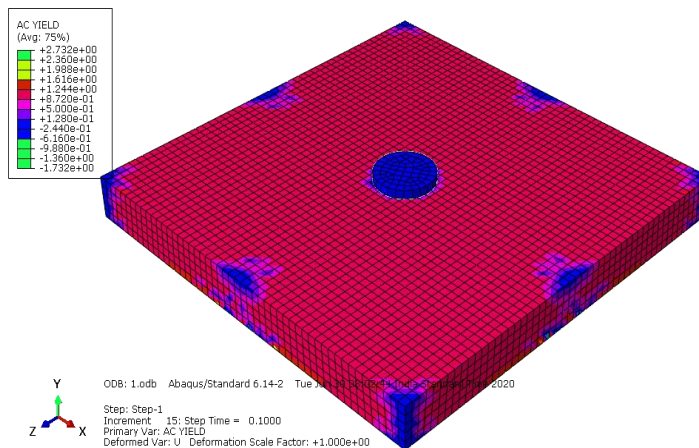
Table 5. Plastic properties used for reinforced bar.

Yield stress (MPa)	Inelastic strain	Yield stress (MPa)	Inelastic strain
400	0	475	0.0007
425	0.0001	487.5	0.0010
450	0.0003	500	0.0020

3.3.1 Finite element analysis results and discussion

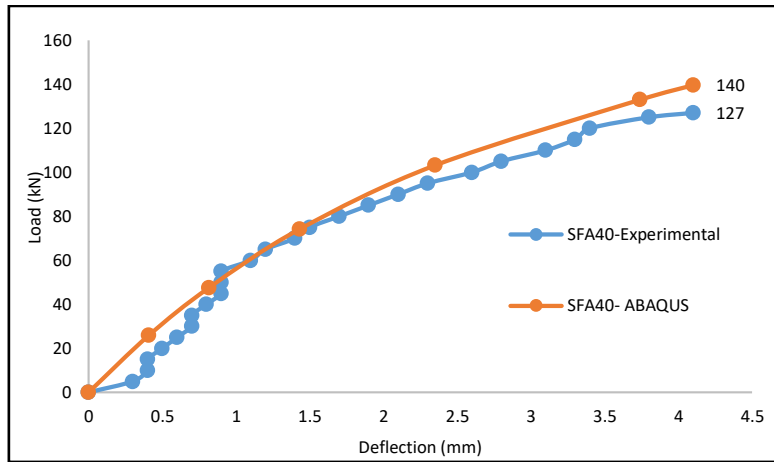
The finite element analysis results give a proper failure mode of the RC slab specimens which will help how the load dissipated to the specimens and the failure behaviour. In general, the loading disc punches the RC slabs at the centre and propagates the punching failure. The punching failure in RC slabs occur when the applied shear force exceeds the concrete mixture shear force. A general failure pattern of RC slabs contains sintered fly ash aggregates and steel fibers was simulated by the ABAQUS was shown in Figure 10.

Figure 10. Failure stage of the RC slabs subjected to punching shear force.

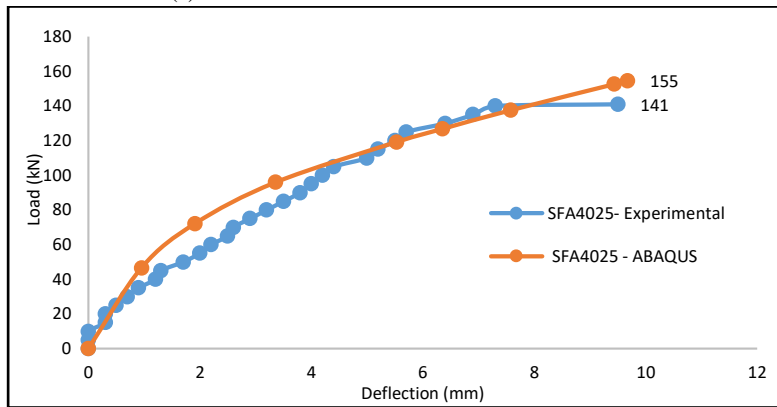


The Figure 10 shows the failure of RC slabs subjected to punching, from this failure we can clearly observe that once a high concentrated force was applied on the top of the slab, the support will be standing alone. The punched slab area will fall down. The red shaded area was the dissipation of shear stress to the supports and the blue shaded area were the slab disjointed from the slab. The Figure 11 shows the comparison of load – deflection curve for the RC slabs subjected to punching for both

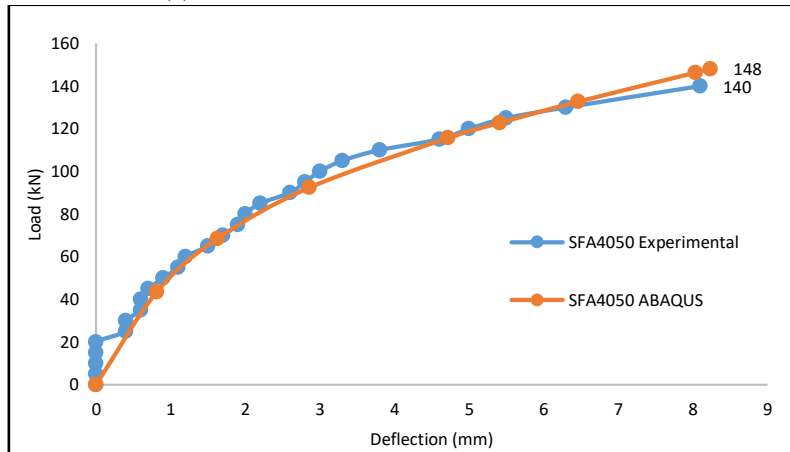
experimental and ABAQUS. The ratio between experimental values and ABAQUS values shown in the Table 6. For all the slab specimens punching shear strength values were correctly predicted by ABAQUS.



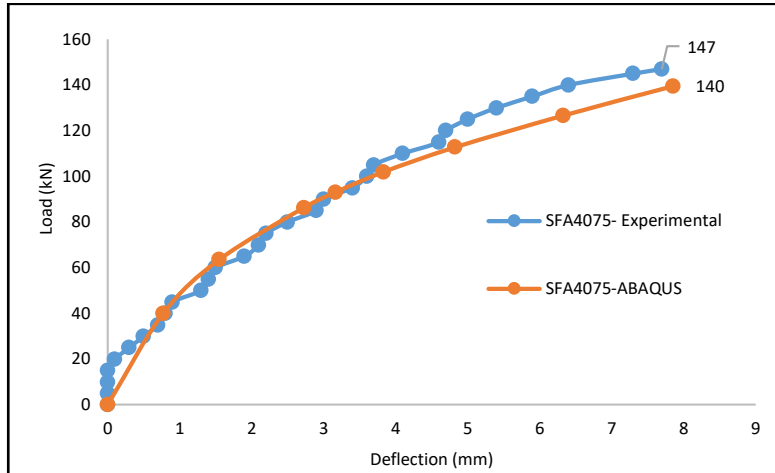
(a). Load – deflection curve for SFA40 RC slab.



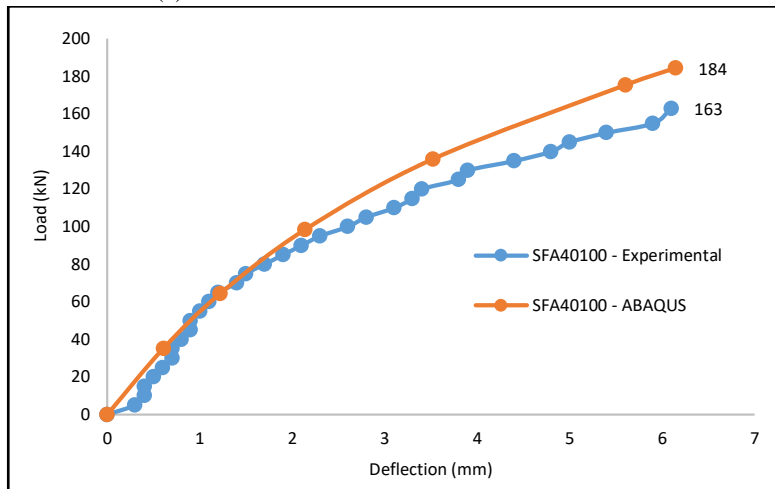
(b). Load – deflection curve for SFA4025 RC Slab.



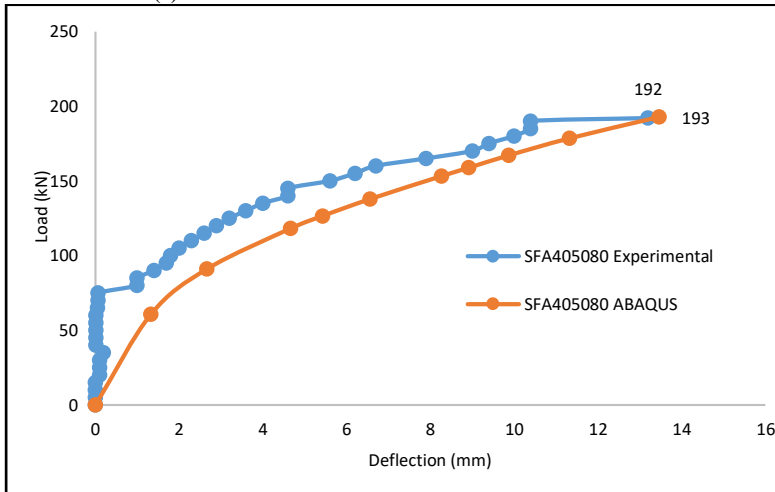
(c). Load – deflection curve for SFA4050 RC Slab.



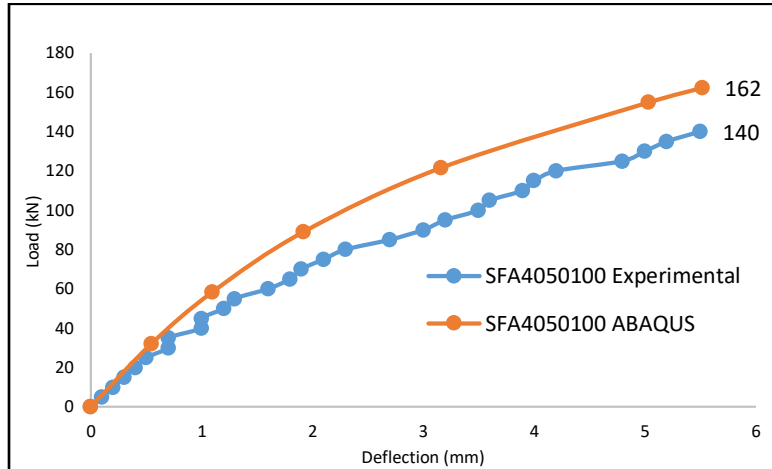
(d). Load – deflection curve for SFA4075 RC Slab.



(e). Load – deflection curve for SFA40100 RC slab.



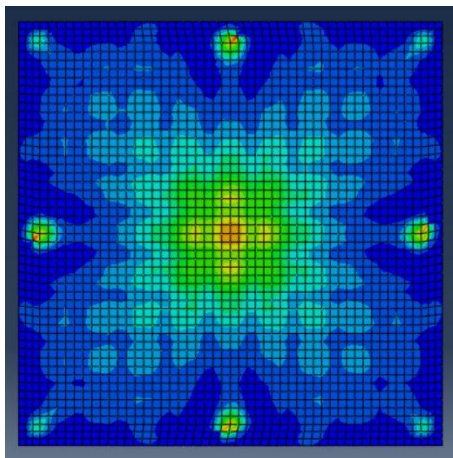
(f) Load – deflection curve for SFA405080 RC Slab.



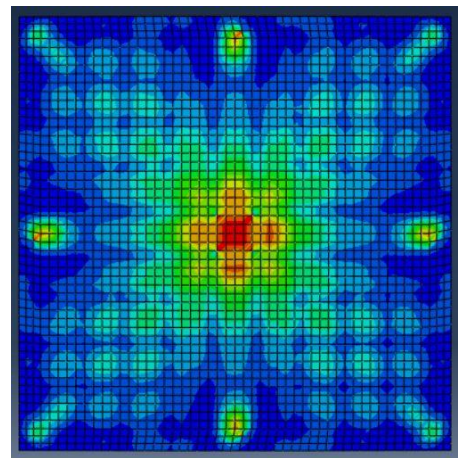
(g) Load – deflection curve for SFA4050100 RC slab.

Figure 11. Load – deflection curves.

The PEMAG of the bottom RC slabs were shown in the Figure 12. The PEMAG shows the failure strains of the RC slabs for all the slabs. It clearly shows that the concrete mixture contains 40 % of sintered fly ash aggregates and steel fibers of volume as 0.25 %, 0.5 % and 0.75 % for the aspect ratio of 55 shows the greater absorption of energy and failure cone at the centre. For the aspect ratio 80 also the same behaviour. For the RC slabs SFA40 concrete contains 40 % sintered fly ash aggregates, the RC slab SFA40100 concrete contains 40 % Sintered fly ash aggregates and the volume of 1.0% of steel fibers for an aspect ratio 55. SFA4050100 concrete contains 40 % sintered fly ash aggregates and 0.5 % of volume steel fibers for an aspect ratio 100 shows the same behaviour. The addition of fibers in concrete slabs was highly depended on the aspect ratio and the volume. The PEMAG gives the failure patterns exactly compared to experimental failure patterns (Genikomsou AS, & Polak MA, 2016). On comparing the PEMAG Figure 12 with experimental failures. The RC slabs fails at centre of the slab and thus it leads to pure punching.



SFA40 - PEMAG



SFA4025 - PEMAG

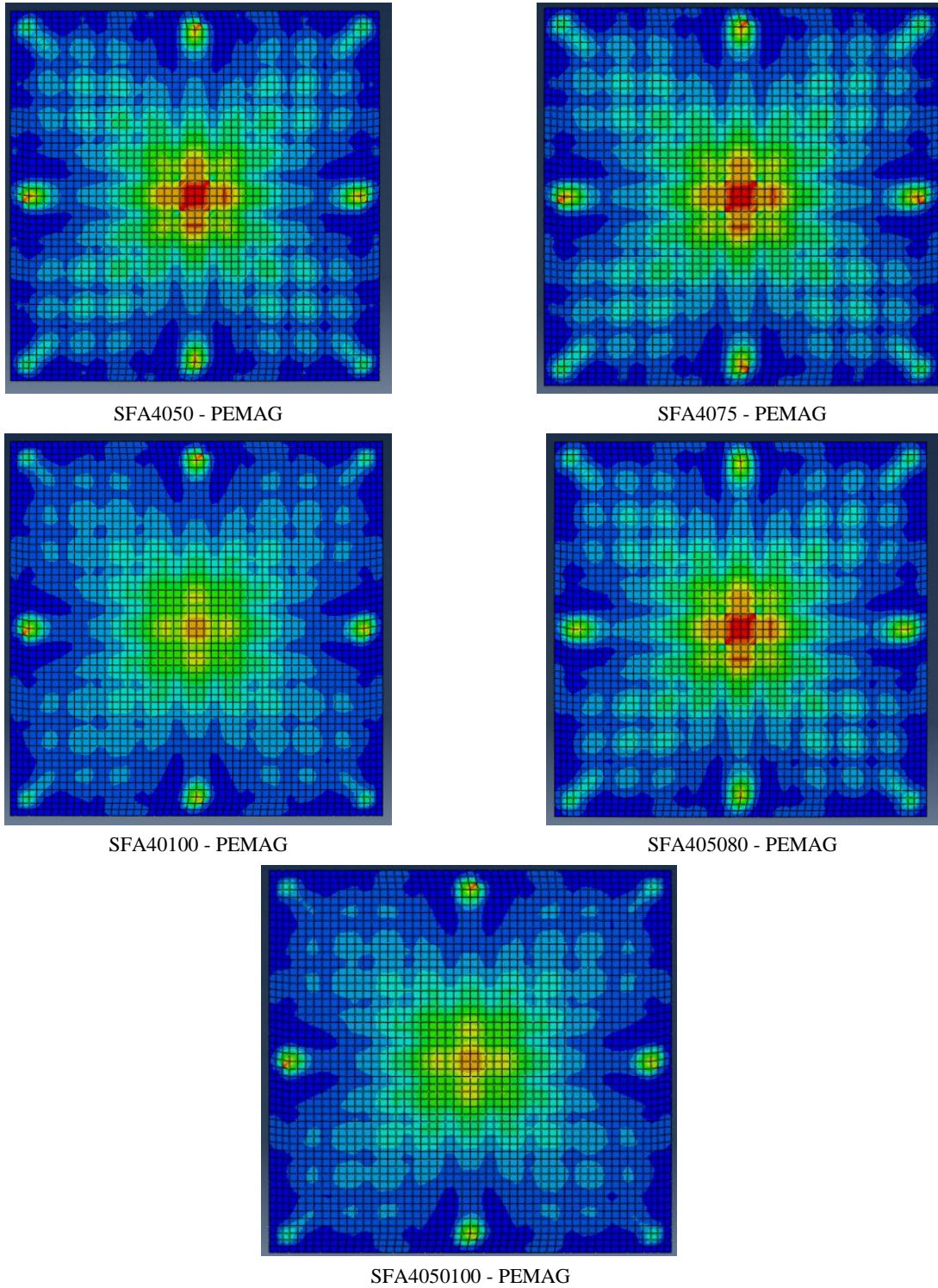


Figure 12. Failure patterns of RC slabs in ABAQUS for different mixtures.

3.4. International design codes and its provisions

Codes of practices of several countries like Indian standard and American concrete institute code present a generalized formula, where the punching load is a product of design nominal shear strength and the area of a chosen critical failure surface. Depending on the code of a country, the critical section for checking punching shear in slabs is taken at 0.5 to 2 times the effective depth from the edge of the load or the reaction.

Generally, the punching shear strength values specified in different codes vary with concrete compressive strength or cylindrical strength. In Indian code IS 456; the punching shear strength is expressed as proportional to $\sqrt{f_{ck}}$. the square root formulae available in the Indian code is adopted from the ACI 318 Code. This international design codes from equations (1) & (2) were used to predict ultimate punching load for the tested slabs. The results are shown in Table 6.

3.4.1 American Concrete Institute Code ACI-318 – 2011

The ultimate Punching shear is the smallest of

$$P_u = 0.17(1 + 2/\beta) \sqrt{f_{cy}} \lambda (b_o \times d) \quad (1a)$$

$$P_u = 0.083((\alpha_s \times d)/b_o) \sqrt{f_{cy}} \lambda (b_o \times d) \quad (1b)$$

$$P_u = 0.33 \sqrt{f_{cy}} \lambda (b_o \times d) \quad (1c)$$

where,

P_u = Ultimate Punching shear strength, kN.

f_{cy} = Cylindrical compressive strength, MPa (Converting by 0.8 times cubical strength)

b_o = Perimeter of critical section (mm), π (Column Diameter + Effective depth); 723 mm

d = Effective depth of the slab (mm)

β = The ratio of long side to short side of the column of the concentrated load.

λ = 1.0 for Normal strength concrete.

α_s = Coefficient depends on the position of the column.

α_s = 40 for inner column, 30 for edge column, 20 for corner column.

3.4.2 Indian Standard Code IS456-2000

As per IS 456: 2000, the expression for calculating the punching shear strength P_u by considering partial safety factor for the material as unity is given by

$$P_u = k_s \times \tau_{uc} \times b_o \times d \quad (2a)$$

Where,

P_u = Ultimate Punching shear strength, kN

$k_s = (0.5 + \beta) < 1$

τ_{uc} = Shear strength in concrete, MPa

$\tau_{uc} = 0.25 \sqrt{f_{ck}}$

f_{ck} = Characteristic compressive strength of concrete, MPa

b_o = Perimeter of critical section (mm), π (Column Diameter + Effective depth); 723 mm

d = Effective depth of the slab (mm).

The comparison between ultimate punching load and predicted from code equations presented in Table 6.

Table 6. Comparison ultimate punching load experimental, international codes and ABAQUS.

Slab names	$\frac{l}{d}$	V_f (%)	Ultimate load (kN)			ABAQUS	Ratio between tested/ABAQUS
			Tested P_u	Predicted by codes			
				P_{ACI}	P_{IS}		
SFA40	-	0 %	127	122	93	140	0.90
SFA4025	55	0.25 %	141	115	87	155	0.91
SFA4050	55	0.5 %	140	120	91	148	0.95
SFA4075	55	0.75 %	140	117	88	147	0.95
SFA40100	55	1.0 %	163	114	86	184	0.89
SFA405080	80	0.5 %	192	118	89	193	0.99
SFA4050100	100	0.5 %	140	115	87	162	0.86

The code results were appropriate if we know the cubical compressive strength of the concrete mixtures. In our concrete mixes, only the direct parameter which we can know was the compressive strength values. To know the real behavior of the RC slabs subjected to punching, an experimental test has to be carried out in the laboratory by making a small-scale specimen, or by using the ABAQUS modelling. Finally, the code book values are only a theoretical value. It will not give the failure modes. It seems that the addition of sintered fly ash aggregates and steel fibers increases the punching shear strength value.

3.5. Theoretical evaluation

The nominal failure moment (M_n) for the RC slabs contains 40 % SFA and different volume with varying aspect ratios of steel fibers was obtained using a theoretical model of their cross -section.

3.5.1 Assumptions in theoretical analysis

The current established model was based on the rectangular stress block. The recommended assumptions can be listed as follows. The adopted stress block was shown in Figure 13. (Basha, Fayed & Mansour, 2020)

- i. Plane sections remains same before bending and after bending.
- ii. The tension force developed in the concrete was ignored.
- iii. An equivalent rectangular stress block was adopted to calculate the compressive force in concrete.
- iv. The partial safety factor for concrete and steel as taken by 1.5 and 1.15.

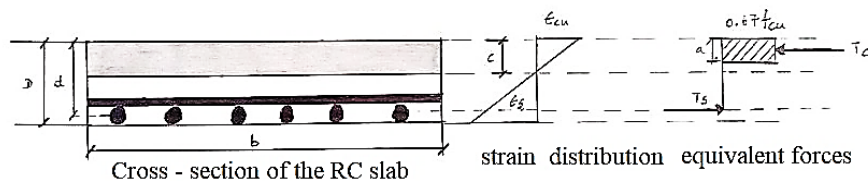


Figure 13. Analytical model for RC slab.

The failure moment of the RC slab section was calculated based on the following equation. The calculate failure punching shear strength and comparison with the experimental values were shown in the Table 7. The failure punching shear calculation was based on the basic structural analysis.

$$M_n = T_s \times \left(d - \frac{a}{2} \right) \quad 3 \text{ (a)}$$

$$c = \left(\frac{A_{st} \times f_y}{0.8 \times 0.67 \times f_{cu} \times b} \right) \quad 3 \text{ (b)}$$

where,

- Mn = Nominal failure moment value
- Ts = Tensile strength of the steel Bars
- d = Effective depth of the RC slab = 80 mm
- a = Height of the rectangular compressive stress block
- c = Location of the neutral axis
- Ast = Area of the steel reinforcement
- fy = Yield strength of the steel bars
- fcu = Cubical compressive strength of the concrete
- b = width of the slab, taken as 1 m

Table 7. Punching shear strength values based on theoretical model.

Slab Designation	P _{u, Exp}	c (mm)	a (mm)	M _n (kN m)	P _{u, the}	P _{u, Exp} / P _{u, the}
SFA40	127	46.78	37.43	41.87	186	0.68
SFA4025	141	53.04	42.43	40.16	179	0.79
SFA4050	140	48.36	38.68	41.44	184	0.76
SFA4075	140	51.34	41.07	40.63	181	0.77
SFA40100	163	53.79	43.03	39.96	178	0.92
SFA405080	192	50.26	40.21	40.92	182	1.05
SFA4050100	140	52.90	42.32	40.20	179	0.78

The punching shear values computed based on the theoretical model shows a reasonable ratio when compared to the experimental punching shear strength value. It varies from 0.68 – 1.05.

4. Conclusion

The study of sintered fly ash aggregates and steel fibers in normal concrete gives the following conclusions,

1. The water absorption of sintered fly ash aggregates was 16.8 % after 24 hrs. While mixing with the concrete it absorbs more water. To avoid this excess absorption, aggregates were used under surface saturated condition;
2. The tested impact and crushing strength values of sintered fly ash aggregates meets the standards of natural aggregates;
3. The partial replacement (by weight) of sintered fly ash aggregates increases the slump values by 1.4, 1.75 and 2.05 times compared to normal concrete slump value;
4. The partial replacement (by weight) of sintered fly ash aggregates increases the compressive strength values by 7.16 %, 27.50 % and 11.30 % compared to normal concrete compressive strength values;
5. The partial replacement (by weight) of sintered fly ash aggregates increases the split tensile strength values by 4.08%, 45.72 % and 14.86 % compared to normal concrete compressive strength values;
6. The replacement of 40 % (by weight) sintered fly ash aggregates in normal concrete increases compressive strength and split tensile strength of the concrete mixtures;
7. The addition of steel fibers in concrete contains 40 % sintered fly ash aggregates and 60 % natural aggregates decreases the slump values linearly as the fiber dosage increases;
8. The incorporation of steel fibers in the concrete mixtures decreases the compressive strength. and split tensile values increase for 0.5 % volume of steel fibers for aspect ratio 55. The short fibers increase the tensile strength;

9. The punching shear strength and energy absorption were high when compared to remaining concrete mixtures. Particularly, the 0.5% steel fibers of aspect ratio 80 performed well;
10. The finite element software ABAQUS gives the same experimental performance for all the concrete mixtures. This can be useful to know how the crack propagates in the RC slabs;
11. The PEMAG represents the failure of the RC slabs in terms of plastic strains;
12. The experimental punching shear strength values were low when compared to IS 456 and ACI 318 predictions;
13. The theoretical model for the RC slabs subjected to punching shear strength was evaluated properly making an assumption. The stress block considered was rectangular shape.

Author contributions: Each author contributed for the design and implementation of the research, for the analysis of the results and to write this manuscript.

Funding: None

Acknowledgments: The author received no financial support for this research, authorship, and/or publication of this article.

Conflicts of interest: The authors declare that they have no conflict of interest.

References

- ABAQUS Theory Manual (6.14), 2014. Dassault Systems, Providence, RI, USA.
- ACI 318-11, Building code Requirements for structural concrete and commentary, 2011.
- Alwash, N. A., & Habbeb, G. (2017). Experimental and Numerical Investigation on The Punching Behavior of High Strength RC Flat Slab Under Repeated Load. *J. Babylon Univ. Eng. Sci.*, 25(2), 479-494.
- Babu B, R. (2021). Experimental and numerical studies on punching shear strength of concrete slabs containing sintered fly ash aggregates. *Revista de la construcción*, 20(1), 15-25.
- Balendran, R. V., Zhou, F. P., Nadeem, A., & Leung, A. Y. T. (2002). Influence of steel fibres on strength and ductility of normal and lightweight high strength concrete. *Building and environment*, 37(12), 1361-1367.
- Bartolac, M., Damjanović, D., & Duvnjak, I. (2015). Punching strength of flat slabs with and without shear reinforcement. *Grđevinar*, 67(08.), 771-786.
- Basha, A., Fayed, S., & Mansour, W. (2020). Flexural strengthening of RC one-way solid slab with Strain Hardening Cementitious Composites (SHCC). *Advances in concrete construction*, 9(5), 511-527.
- Caratelli, A., Imperatore, S., Meda, A., & Rinaldi, Z. (2016). Punching shear behavior of lightweight fiber reinforced concrete slabs. *Composites Part B: Engineering*, 99, 257-265.
- CEB - FIB model code for concrete structures 2010. Ernst & sohn; 2013.
- Cheeseman, C. R., Makinde, A., & Bethanis, S. (2005). Properties of lightweight aggregate produced by rapid sintering of incinerator bottom ash. *Resources, Conservation and Recycling*, 43(2), 147-162.
- Divyah, N., Thenmozhi, R., & Neelamegam, M. (2020). Experimental and Numerical Analysis of Battered Built-up Lightweight Concrete Encased composite columns subjected to axial cyclic loading. *Latin American Journal of Solids and Structures*, 17.
- Genikomsou, A. S., & Polak, M. A. (2015). Finite element analysis of punching shear of concrete slabs using damaged plasticity model in ABAQUS. *Engineering Structures*, 98, 38-48.
- Genikomsou, A. S., & Polak, M. A. (2016). Finite-element analysis of reinforced concrete slabs with punching shear reinforcement. *Journal of Structural Engineering*, 142(12), 04016129.
- Gesoğlu, M., Güneyisi, E., Mahmood, S. F., Öz, H. Ö., & Mermerdaş, K. (2012). Recycling ground granulated blast furnace slag as cold bonded artificial aggregate partially used in self-compacting concrete. *Journal of hazardous materials*, 235, 352-358.
- Gomathi, P., & Sivakumar, A. (2015). Accelerated curing effects on the mechanical performance of cold bonded and sintered fly ash aggregate concrete. *Construction and building Materials*, 77, 276-287.
- Güneyisi, E., Gesoğlu, M., Pürsünlü, Ö., & Mermerdaş, K. (2013). Durability aspect of concretes composed of cold bonded and sintered fly ash lightweight aggregates. *Composites Part B: Engineering*, 53, 258-266.

- Harajli, M. H., Maalouf, D., & Khatib, H. (1995). Effect of fibers on the punching shear strength of slab-column connections. *Cement and Concrete Composites*, 17(2), 161-170.
- IS 10262: 2009, Concrete Mix Proportioning – Guidelines, Bureau of Indian Standards. New Delhi-12.
- IS 2386, Methods of test for aggregates for concrete, Bureau of Indian Standards. New Delhi, 1963 [Reaffirmed in 2002].
- IS 456-2000, Indian standard code of practice for plain and reinforced concrete, 2000.
- IS: 2386, Indian Standard Specification, Methods of Test for Aggregates for Concrete: Part 3, Specific Gravity, Density, Voids, Absorption and Bulking, Bureau of Indian Standards, New Delhi, 1963 [Reaffirmed in 2002].
- IS: 2386, Indian Standard Specification, Methods of Test for Aggregates for Concrete: Part 4, Mechanical Properties Bureau of Indian Standards, New Delhi, 1963 [Reaffirmed in 2002].
- IS: 2386, Indian Standard Specification, Methods of Test for Aggregates for Concrete: Part 1 Particle Size and Shape, Bureau of Indian Standards, New Delhi, 1963 [Reaffirmed in 2002].
- Kayali, O., Haque, M. N., & Zhu, B. (1999). Drying shrinkage of fibre-reinforced lightweight aggregate concrete containing fly ash. *Cement and concrete research*, 29(11), 1835-1840.
- Kearsley, E. P., Wainwright, P. J., & Amtsbuchler, R. (2003). The effect of fly ash properties on concrete strength In *Journal of the South African Institution of Civil Engineering*, 45 (1) 2003, pp. 19-24: discussion. *Journal of the South African Institution of Civil Engineering, Joernaal van die Suid-Afrikaanse Instituut van Siviele Ingenieurswese*, 45(4), 18-19.
- Kearsley, Elsabé & Elsaigh, W. (2003). Effect of ductility on load-carrying capacity of steel fibre reinforced concrete ground slabs. *Journal of the South African Institution of Civil Engineers*. 45. 25-30.
- Kockal, N. U., & Ozturan, T. (2011). Durability of lightweight concretes with lightweight fly ash aggregates. *Construction and Building Materials*, 25(3), 1430-1438.
- Kuang, J. S., & Morley, C. T. (1993). Punching shear behavior of restrained reinforced concrete slabs. *Structural Journal*, 89(1), 13-19.
- Mahmoud, Z. I., El tony, E. tony M., & Saeed, K. S. (2018). Punching shear behavior of recycled aggregate reinforced concrete slabs. *Alexandria Engineering Journal*, 57(2), 841–849.
- Mohammadi, Y., Singh, S. P., & Kaushik, S. K. (2008). Properties of steel fibrous concrete containing mixed fibres in fresh and hardened state. *Construction and Building Materials*, 22(5), 956-965.
- Nadesan, M. S., & Dinakar, P. (2017). Mix design and properties of fly ash waste lightweight aggregates in structural lightweight concrete. *Case studies in construction materials*, 7, 336-347.
- Nadesan, M. S., & Dinakar, P. (2017). Structural concrete using sintered fly ash lightweight aggregate: A review. *Construction and Building Materials*, 154, 928-944.
- Nemani, R. D. M., Rao, M. V. S., & Grandhe, V. V. S. N. (2016). Studies on Punching Shear Resistance of Two-Way Slab Specimens with Partial Replacement of Cement by GGBS with Different Edge Conditions. *Journal of The Institution of Engineers (India): Series A*, 97(3), 307-312.
- Nguyen-Minh, L., Rovňák, M., Tran-Quoc, T., & Nguyenkim, K. (2011). Punching shear resistance of steel fiber reinforced concrete flat slabs. *Procedia Engineering*, 14, 1830-1837.
- Patra, S. N., Patra, R. K., Mukharjee, B. B., & Jena, S. (2021). Development of sustainable concrete incorporating metakaolin and sintered fly ash aggregate. *Structural Concrete*.
- Reis, N., de Brito, J., Correia, J. R., & Arruda, M. R. (2015). Punching behaviour of concrete slabs incorporating coarse recycled concrete aggregates. *Engineering structures*, 100, 238-248.
- Sermet, F., & Ozdemir, A. (2016). Investigation of punching behaviour of steel and polypropylene fibre reinforced concrete slabs under normal load. *Procedia engineering*, 161, 458-465.
- Shah, S. P., Daniel, J. I., Ahmad, S. H., Arockiasamy, M., Balaguru, P. N., Ball, C. G., & Zollo, R. F. (1993). Guide for specifying, proportioning, mixing, placing, and finishing steel fiber reinforced concrete. *ACI Materials Journal*, 90(1), 94-101.
- Subramanian, N. (2005). Evaluation and enhancing the punching shear resistance of flat slabs using HSC. *The Indian Concrete Journal*, 79(4), 31-37.
- Tuğrul Erdem, R. (2021). Dynamic responses of reinforced concrete slabs under sudden impact loading. *Revista de la construcción*, 20(2), 346-358.
- Wainwright, P. J., & Robery, P. (1997). Structural performance of reinforced concrete made with sintered ash aggregate. *Studies in environmental science*, 411-419.
- Youm, K. S., Kim, J. J., & Moon, J. (2014). Punching shear failure of slab with lightweight aggregate concrete (LWAC) and low reinforcement ratio. *Construction and Building Materials*, 65, 92-102.



Copyright (c) 2022 Ranjith Babu, B., and Thenmozhi, R. This work is licensed under a [Creative Commons Attribution-NonCommercial-No Derivatives 4.0 International License](https://creativecommons.org/licenses/by-nc-nd/4.0/).